Biosensors and Bioelectronics 65 (2015) 103–107

Contents lists available at ScienceDirect

Biosensors and Bioelectronics

journal homepage: www.elsevier.com/locate/bios

Labeling-free fluorescent detection of DNA hybridization through FRET from pyrene excimer to DNA intercalator SYBR green I

Ruyi Zhou, Chen Xu, Jie Dong, Guojie Wang*

School of Materials Science and Engineering, University of Science and Technology Beijing, Beijing 100083, China

ARTICLE INFO

Article history:
Received 25 July 2014
Received in revised form
8 October 2014
Accepted 13 October 2014
Available online 18 October 2014

Keywords:
Biosensor
DNA hybridization
Fluorescence
FRET
Pyrene excimer

ABSTRACT

A novel labeling-free fluorescence complex probe has been developed for DNA hybridization detection based on fluorescence resonance energy transfer (FRET) mechanism from pyrene excimer of pyrene-functionalized poly [2-(*N*, *N*-dimethylamino) ethyl methacrylate] (PFP) to SYBR Green I (SG, a specific intercalator of double-stranded DNA) in a cost-effective, rapid and simple manner. The complex probe consists of the positively charged PFP, SG and negatively charged single-stranded DNA (ssDNA). Upon adding a complementary strand to the complex probe solution, double-stranded DNA (dsDNA) was formed, followed by the intercalation of SG into dsDNA. The pyrene excimer emission was overlapped with the absorption of SG very well and the electrostatic interactions between PFP and dsDNA kept them in close proximity, enabling efficient FRET from pyrene excimer to SG. The fluorescence of SG in the duplex DNA resulting from FRET can be successfully applied to detect DNA hybridization with high sensitivity for a very low detection limit of 10 nM and excellent selectivity for detection of single base pair mismatch.

1. Introduction

During the past decades, the sequence-specific DNA detection has received great attention because of its application in many areas, such as clinical diagnosis, gene expression analysis, biomedical studies (Bi et al., 2010; Rosi et al., 2006; Sefah et al., 2009; Zheng et al., 2013b; Zhu et al., 2010). Various techniques for DNA detection have been developed, such as electrochemical (Ahangar and Mehrgardi, 2012; Ganguly et al., 2009; Qiu et al., 2011; Cheng et al., 2014) and fluorescent (Kang et al., 2009, 2010; Lee et al., 2014; Xiang et al., 2012; Zhang and Zhou, 2012) methods. Homogeneous DNA hybridization assays based on fluorescence resonance energy transfer (FRET) between energy-transfer chromophore pairs are attractive because of their simplicity of operation and use of standard optical equipment (Wang et al., 2011). Recently, the FRET strategy employing water-soluble cationic conjugated polymers (CCP) with a large number of chromophoric repeat units, which enable the transfer of excitation energy along the whole backbone of the CCP to the reported chromophore via FRET, has been paid more attention for DNA detection with high sensitivity and selectivity (Feng et al., 2011; Jiang et al., 2009; Liu et al., 2014; Xu et al., 2005, 2010). Bazan and co-workers designed a three-color DNA detection assay with CCP and a fluorophore-labeled peptide nucleic acid strand through efficient FRET from CCP to the fluorophore (Liu and Bazan, 2004). Wang and co-workers demonstrated a simple method using CCP, EB and fluorescein-labeled ssDNA for DNA detection based on two FRET process from CCP to fluorescein and then to EB with enhanced detection efficiency (Feng et al., 2008; Tian et al., 2007). In these assays, the fluorophore moieties as acceptors were covalently linked to the DNA or PNA probes and the negatively charged phosphate groups of the DNA interacted with CCP to form the complexes by electrostatic interactions, which could detect DNA hybridization through FRET from CCP to the fluorophore labeled at the end of nucleic acids. However, labeling process with chromophores is high-cost, complex and time-consuming, which may limit its applications in detection of nucleic acids (Ma et al., 2013; Pu and Liu, 2009; Wang et al., 2011). Thus, to overcome the aforementioned limitations, development of novel and simple labeling-free FRET probes for DNA detection is highly desirable.

The labeling-free assays using DNA intercalators can exhibit high sensitivity and selectivity with low cost and convenient operation (Aied et al., 2012; Lin et al., 2015; Pu and Liu, 2009; Wang et al., 2011, 2014; Xu et al., 2010). SYBR Green I (SG), a DNA intercalating dye, is an asymmetrical cyanine dye and has a significantly enhanced fluorescence in complex with dsDNA due to a dampening of its intra-molecular motions (Dragan et al., 2012), which can be potentially utilized to develop labeling-free sensors for DNA hybridization detection. In addition, SG has a high quantum yield of 0.80 that is 100 times larger than that of the other

* Corresponding author.
E-mail address: guojie.wang@mater.ustb.edu.cn (G. Wang).

http://dx.doi.org/10.1016/j.bios.2014.10.029
0956-5663/

commonly used intercalating dye EB, which is also much less mutagenic than EB (Lee et al., 2008). Thus, SG has been widely used for the selective detection of metal ions (K^+, Hg^{2+} etc.) (Liu, 2008; Xu et al., 2010) and biological molecules (DNA, proteins etc.) (Li et al., 2013; Zheng et al., 2013a) with low cost in a "mix-and-detect" manner. For example, Zheng and co-workers developed a labeling-free signal amplification assay for DNA detection based on exonuclease III and SG, which showed excellent detection selectivity for single-base discrimination.

Recently, we designed a labeling-free fluorescent complex probe composed of pyrene-functionalized water-soluble cationic polyelectrolytes and ssDNA for DNA hybridization detection based on a decreased fluorescence resulted from the intercalation of pyrene into the duplex DNA (Yang et al., 2012; Zhang et al., 2013; Zhao et al., 2013), while the fluorescence turn-off assay for hybridization detection might limit the sensitivity and selectivity. Herein, to improve the detection sensitivity and selectivity, we develop a novel labeling-free DNA complex probe composed of a water-soluble positively charged pyrene-functionalized PDMAEMA (PFP), DNA intercalator SG, and negatively charged ssDNA for detection of DNA hybridization through efficient FRET from pyrene excimer of PFP to SG. The novel probe shows high sensitivity with a 10 nM detection limit of the target DNA and excellent selectivity for single base mismatch detection, which provides great potential in DNA hybridization detection. This proposed strategy exhibits several advantages over existing techniques such as simple and low-cost in design, fast in operation and high specific as compared to the previously reported methods using fluorescent labeling DNA probe, which might provide a promising sensing platform for bioanalysis, clinical molecular diagnostics and environmental monitoring.

2. Materials and methods

2.1. Materials and apparatus

Phosphorous tribromide (98.5%) from Sinopharm Chemical Reagent Co. Ltd., 1-pyrenemethanol (99%), 2-(Dimethylamino) ethyl methacrylate (99%), ethyl 2-bromoisobutyrate (98%), copper bromide (98%), 1.1.4.7.10.10-hexamethyltriethylenetetramine (97%) from Aldrich and the conventional reagents were used as received. All atmosphere sensitive reactions were done under nitrogen. Deionized water was obtained from a Millipore water purification system. SG was purchased from Life Technologies. The HPLC-purified single stranded DNAs (ssDNAs) and phosphate buffer solution used in this work were obtained from the Shanghai Sangon Biological Engineering Technology & Services Co. Ltd. (Shanghai, China). The sequences of the DNA oligonucleotides were as follows:

ssDNA$_1$: 5′-CAA GTA GAA TGT ATG TGC-3′
ssDNA2: 5′-GCA CAT ACA TTC TAC TTG-3′
ssDNA1nc: 5′-GCA CAT A**T**A TTC TAC TTG-3′
ssDNA2nc: 5′-GCA CA**G** ACA TTC **A**AC TTG-3′
ssDNA3nc: 5′-GCA **G**AT AC**C** TTC TA**A** TTG-3′
ssDNAa: 5′-AAA AAA AAA AAA AAA AAA-3′
ssDNAt: 5′-TTT TTT TTT TTT TTT TTT-3′
ssDNAc: 5′-CCC CCC CCC CCC CCC CCC-3′

Here ssDNA$_2$ is complementary with ssDNA$_1$; ssDNA$_{1nc}$, ssDNA$_{2nc}$ and ssDNA$_{3nc}$ are single-mismatched, double-mismatched and triple-mismatched DNAs with ssDNA$_1$, respectively; ssDNA$_a$, ssDNA$_c$ and ssDNA$_t$ are non-complementary ssDNAs.

^{1}H-NMR spectra were recorded from $CDCl_3$ solution on a Bruker AM 400 spectrometer. The molecular weight of the polymer was determined by gel permeation chromatography (GPC) (Waters 1515) with styragel columns relative to polystyrene standards using THF as eluent. UV–visible absorption spectra were taken using a Shimadzu UV-3100 UV–vis spectrophotometer. The fluorescence spectra were measured on a Hitachi F-4500 spectrofluorometer, in which all the measurements were done in 10 mM phosphate buffer solutions (pH=7.4).

2.2. Polymer synthesis

First, the polymer PDMAEMA was synthesized by atom transfer radical polymerization (ATRP). The number-average molecular weight (Mn) and polydispersity index (PDI) of the polymer were determined to be 2.32×10^4 and 1.09, respectively, by GPC. Next, 1-(Bromomethy) pyrene was synthesized and incorporated into PDMAEMA through quaternization with the dimethylaminoethyl unit to achieve the pyrene-functionalized PDMAEMA.

2.3. Sample preparation

The complex probes were prepared by dissolving a suitable amount of the polymer PFP in phosphate buffer solution (10 mM, pH=7.4), following addition of SG and ssDNA$_1$. Complementary or non-complementary ssDNAs with equal amount to ssDNA$_1$was mixed with the complex probe to investigate its fluorescence changes. All the samples containing DNA were annealed at 90 °C for 10 min and slowly cooled down to room temperature prior to measurement.

3. Results and discussion

The water soluble fluorescent pyrene-functionalized PDMAEMA was synthesized through the quaternization of the dimethylaminoethyl units of the polymer PDMAEMA with 1-(bromomethy) pyrene. The detailed procedure of the synthesis can be found in the Supporting Information. In this work, the polymer PDMAEMA was synthesized by atom transfer radical polymerization (ATRP). The number-average molecular weight (Mn) and polydispersity index (PDI) of the polymer were determined to be 2.32×10^4 and 1.09, respectively, by gel permeation chromatography (GPC). Here a pyrene-functionalized polymer PFP with a functionalization degree of 13.0% was used to form the complex probe. The fluorescence quantum yield (Φ_F) of PFP was determined to be 0.081, using quinine sulfate in sulfuric acid (1.0 N) as a reference (Φ_R=0.55). Scheme 1 shows the chemical structures of the

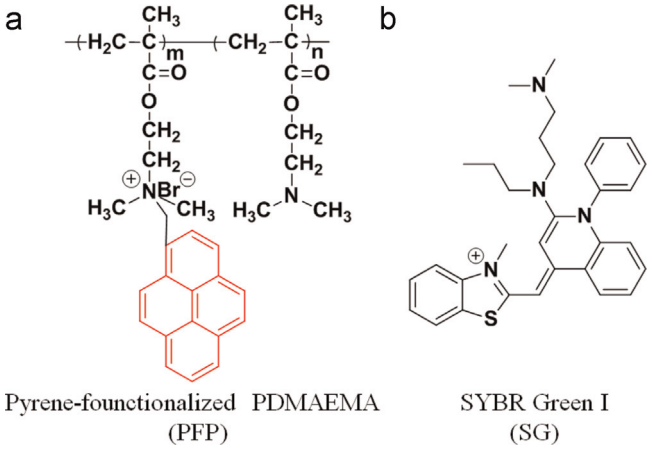

Scheme 1. Chemical structures of PFP (a) and SG (b).

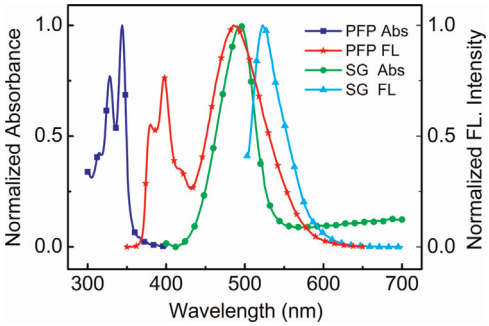

Fig. 1. Normalized UV–vis absorption and fluorescence emission spectra of PFP (1×10^{-5} M, excited at 344 nm) and SG (3×10^{-6} M, excited at 490 nm) in phosphate buffer (10 mM, pH=7.4).

pyrene-functionalized polymer PFP and the DNA intercalating dye SG.

In this work, we used pyrene excimer of the pyrene-functionalized polymer PFP as the energy donor and SG as the energy acceptor for FRET. The absorption and fluorescence spectra of PFP and SG in PBS buffer are shown in Fig. 1. The two fluorescence bands in the wavelength ranges of 360–410 nm and 420–600 nm are attributed to the pyrene monomer emission and excimer emission, respectively (Wang et al., 2009). It should be noted that the excimer emission band of the polymer PFP overlaps the absorption band of SG very well. The sufficient spectral overlap between the donor and acceptor may guarantee an efficient energy transfer from PFP to SG.

Scheme 2 illustrates the mechanism of the fluorescent complex probe for labeling-free detection of DNA hybridization through FRET. In the presence of complementary ssDNA, the double-stranded DNA will be formed and SG molecules can intercalate into the formed dsDNA through intercalation interactions. The electrostatic interactions between the polycation PFP and the polyanion dsDNA may keep the fluorescent polymer PFP and SG in close proximity, and the excimer emission and absorption of SG overlaps very well shown in Fig. 1, thus the efficient FRET fluorescence of SG can be observed. In the presence of non-complementary ssDNA, the double-stranded DNA will not be formed and the intercalation of SG will not occur, thus, the FRET fluorescence of SG can not be detectable because of the quenching of SG in its free state (Dragan et al., 2012).

Fig. 2a exhibits the fluorescent emission spectra of PFP/ssDNA$_1$/SG complex probe with different concentrations of SG (i.e., 1 μM, 2 μM, and 3 μM) in the presence of the complementary ssDNA$_2$ in phosphate buffer (10 mM, pH=7.4), excited at the absorption wavelength (344 nm) of PFP. With the increase of the concentration of SG, the pyrene excimer emission centered around 480 decreased and the SG emission centered around 525 nm increased. The appearance of SG emission and the decrease of pyrene excimer emission when excited at the absorption wavelength of PFP, where SG has negligible absorption, confirmed the FRET from pyrene excimer to SG in the system. In addition, it can also be seen that the emission of SG was broadened and bathochromic shifted (from 520 to 528 nm) when SG concentration increased from 1 μM to 3 μM, resulting from the nonspecific binding of SG to the DNA strands (Lee et al., 2008). Fig. 2b provides the fluorescence intensity ratio of SG to pyrene excimer (I_{SG}/I_{EX}) of PFP/ssDNA$_1$/SG complex probe in the presence of the complementary ssDNA$_2$ with different concentrations of SG, from which it can be seen that the fluorescence intensity ratio was the largest when the concentration of SG was 3 μM due to the efficient energy transfer from PFP to SG. Thus the concentration of SG with 3 μM was used to investigate the detection selectivity and sensitivity in this work.

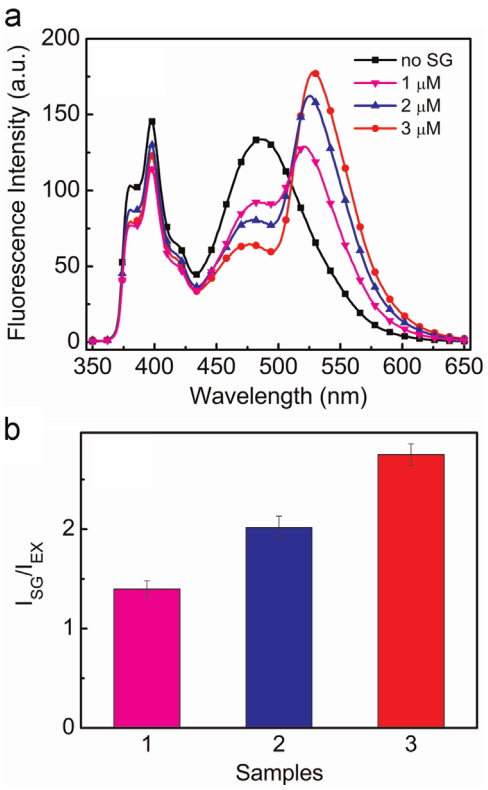

Fig. 2. Fluorescence emission spectra (a) and fluorescence intensity ratio of SG to pyrene excimer (I_{SG}/I_{EX}) (b) of PFP/dsDNA/SG as a function of SG concentration: 1 μM, 2 μM, 3 μM. λ_{ex}=344 nm, [PFP]=1×10^{-5} M, [ssDNA$_1$]=[ssDNA$_2$]=1×10^{-6} M, in phosphate buffer (10 mM, pH=7.4). Each error bar indicates the standard deviation and the relative standard deviation is less than 5.9%.

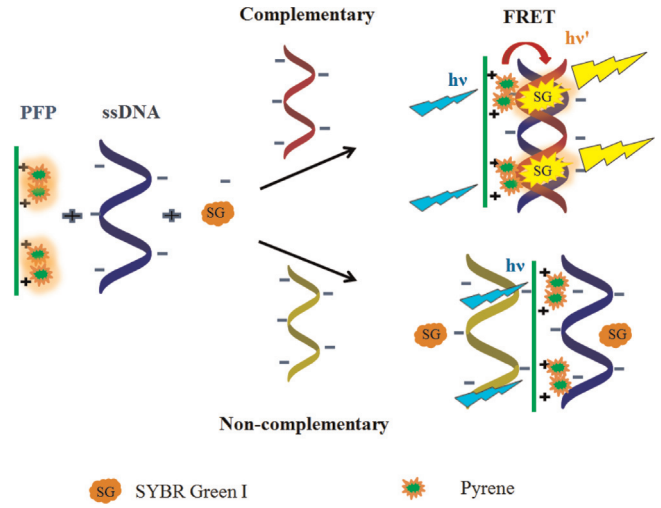

Scheme 2. Schematic representation of the fluorescent complex probe for labeling-free detection of DNA hybridization through FRET.

To evaluate the selectivity of the complex probe, its fluorescence in the presence of complementary ssDNA$_2$ and non-complementary ssDNA such as ssDNA$_{1nc}$, ssDNA$_{2nc}$, ssDNA$_{3nc}$, and ssDNA$_{a(/c/t)}$ was explored. Fig. 3a shows the emission spectra of the complex probe composed of PFP, ssDNA$_1$ and SG upon adding complementary or non-complementary target DNA at the concentration of 1.0×10^{-6}M. Upon adding the non-complementary DNA such as ssDNA$_a$, ssDNA$_c$ and ssDNA$_t$, only a little increase of fluorescence intensity of SG could be seen, while upon adding the triple-mismatched ssDNA$_{3nc}$, double-mismatched ssDNA$_{2nc}$, single-mismatched ssDNA$_{1nc}$ and complementary ssDNA$_2$, the

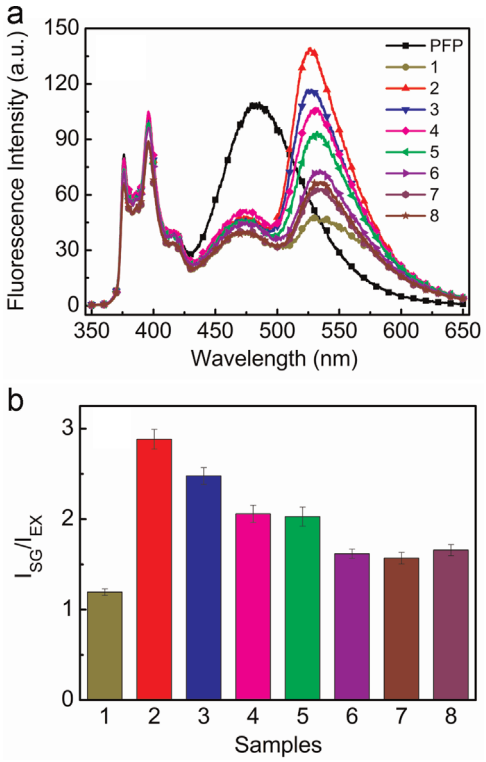

Fig. 3. Fluorescence emission spectra (a) and the fluorescence intensity ratio of SG to pyrene excimer (I_{SG}/I_{EX}) (b) from solutions containing PFP, complex probe (PFP/ssDNA$_1$/SG) (1), PFP/dsDNA/SG (2), PFP/(ssDNA$_1$+ssDNA$_{1nc}$)/SG (3), PFP/(ssDNA$_1$+ssDNA$_{2nc}$)/SG (4), PFP/(ssDNA$_1$+ssDNA$_{3nc}$)/SG (5), PFP/(ssDNA$_1$+ssDNA$_a$)/SG (6), PFP/(ssDNA$_1$+ssDNA$_c$)/SG (7), and PFP/(ssDNA$_1$+ssDNA$_t$)/SG (8) in phosphate buffer (10 mM, pH=7.4). λ_{ex}=344 nm, [PFP]=1×10^{-5} M, [ssDNAx]=1.0×10^{-6} M, [SG]=3×10^{-6} M. Each error bar indicates the standard deviation and the relative standard deviation is less than 5.1%.

fluorescence intensity of SG increased significantly with the increase of the matched degree. It should be noted that the difference in FRET fluorescence of SG was quite clear even when the probe encountered the single-mismatched ssDNA$_{1nc}$ and the complementary ssDNA$_2$. However, for the probe using SG only, SG showed strong background fluorescence and the fluorescence intensity when mixed with one-base mismatched DNA could not be distinguished from that when mixed with the complementary DNA (Fig. S4, Supporting Information).

Fig. 3b demonstrates the fluorescence intensity ratio of SG to pyrene excimer (I_{SG}/I_{EX}) upon adding ssDNA$_2$, ssDNA$_{1nc}$, ssDNA$_{2nc}$, ssDNA$_{3nc}$ and ssDNA$_{a(/c/t)}$ to the complex probe, from which it can be clearly seen that the fluorescence intensity ratio (I_{SG}/I_{EX}) increased with the increase of the matched degree, following the order of ssDNA$_{a(/c/t)}$ < ssDNA$_{3nc}$ < ssDNA$_{2nc}$ < ssDNA$_{1nc}$ < ssDNA$_2$. Both the fluorescence intensity of SG and the fluorescence intensity ratio of SG to pyrene excimer (I_{SG}/I_{EX}) in the presence of complementary ssDNA were quite distinct from those in the presence of single-mismatched ssDNA. Therefore, the complex probe composed of the fluorescent polymer PFP and SG exhibited an excellent selectivity for detection of single nucleotide mismatch.

In addition, to investigate the sensitivity of the complex probe for detection of DNA hybridization, the emission spectra of the complex probe (PFP/ssDNA$_1$/SG) were investigated under the different concentrations of complementary ssDNA$_2$ and non-complementary DNA strands (i.e., ssDNA$_{1nc}$, ssDNA$_{3nc}$, ssDNA$_a$), excited at the absorption wavelength of pyrene (344 nm), see the Supporting Information (Fig. S3). Fig. 4 shows the fluorescence intensity ratio of SG to pyrene excimer (I_{SG}/I_{EX}) as a function of the concentration of the target DNA, from which it can be seen that

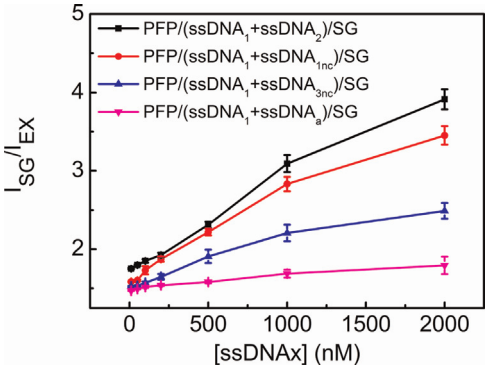

Fig. 4. Fluorescence intensity ratio of SG to pyrene excimer (I_{SG}/I_{EX}) for the complex probe (PFP/ssDNA$_1$/SG) as a function of concentration of ssDNA$_2$, ssDNA$_{1nc}$, ssDNA$_{3nc}$, and ssDNA$_a$. λ_{ex}=344 nm, [PFP]=1.0×10^{-5} M, [ssDNA$_1$]=1.0×10^{-6} M, [SG]=3.0×10^{-6} M, in PBS buffer (10 mM, pH=7.4). Each error bar indicates the standard deviation and the relative standard deviation is less than 6.1%.

the fluorescence intensity ratio increased with the increase of the concentration of target DNA. For the non-complementary ssDNA$_a$, the ratio I_{SG}/I_{EX} was very low and increased little with the increase of its concentration; while for the triple-mismatched ssDNA$_{3nc}$, single-mismatched ssDNA$_{1nc}$ and complementary ssDNA$_2$, the ratio I_{SG}/I_{EX} increased with the increase of their concentrations significantly. The more the matched base pairs, the higher the FRET fluorescence intensity ratio I_{SG}/I_{EX}. It should be noted that the single-mismatched and complementary ssDNAs could be still distinguished when their concentrations were as low as 10 nM, indicating that the complex probe composed of the fluorescent polymer PFP and SG could be used for DNA hybridization detection with high sensitivity.

In addition, the strategy for detection of DNA sequences based on the FRET fluorescence change can be still practical when the DNA sequence contains more bases. Fig. S5 (Supporting Information) shows that the fluorescence changes of the complex probe composed of a DNA with 30 bases could be used to distinguish the complementary DNA from the non-complementary DNA. As shown in Fig. 4 and S5, the signal value of I_{SG}/I_{EX} is dependent not only on the mismatch but also on the concentration and length of target DNA. Moreover, the fluorescence changes of the complex probe (PDF/ssDNA$_1$/SG) when mixed with one-base mismatched ssDNA$_{1nc-1}$ (5′-GCA CAT ACA TTC TAC T**C**G-3′), ssDNA$_{1nc-2}$ (5′-GCA CAT ACA TTC T**G**C TTG-3′) and ssDNA$_{1nc-3}$ (5′-GCA CAT A**T**A TTC TAC TTG-3′) with different mismatch positions were also explored, shown in Fig. S6 (Supporting Information), from which it can be seen that the fluorescence intensity decreased when the mismatch moved away from the termini of target DNA, resulted from the decreased stability of the duplexes (Igloi, 1998).

4. Conclusion

In conclusion, we developed a novel labeling-free complex probe composed of a fluorescent positively charged pyrene-functionalized PDMAEMA (PFP), a single strand DNA and a DNA intercalating dye SG, i.e. PFP/ssDNA/SG system, which could detect DNA hybridization through FRET from the donor pyrene excimer of PFP to the acceptor SG. The changes in FRET fluorescence intensity ratio of SG to pyrene excimer (I_{SG}/I_{EX}) were used to detect the DNA hybridization. The more the matched base pairs, the higher the FRET fluorescence intensity ratio I_{SG}/I_{EX}. The complementary DNA can be clearly distinguished from the single-mismatched with very low detection limit of 10 nM,

demonstrating the high sensitivity and selectivity of the complex probe, which may find wide applications in optical biosensing.

Acknowledgment

This work was supported by the National Natural Science Foundation of China (Grant nos. 21074010 and 51373025), Beijing Municipal Natural Science Foundation (Grant no. 2112029), the Program for New Century Excellent Talents in University (NCET-11-0582), and the Fundamental Research Funds for the Central Universities (FRE-TP-12-004B).

Appendix A. Supplementary Information

Supplementary data associated with this article can be found in the online version at doi: http://dx.doi.org/10.1016/j.bios.2014.10.029.

References

Ahangar, L.E., Mehrgardi, M.A., 2012. Biosens. Bioelectron. 38, 252–257.
Aied, A., Zheng, Y., Pandit, A., Wang, W.X., 2012. ACS Appl. Mater. Inter. 4, 826–831.
Bi, S., Zhang, J.L., Zhang, S.S., 2010. Chem. Commun. 46, 5509–5511.
Cheng, W., Zhang, W., Yan, Y.R., Shen, B., Zhu, D., Lei, P.H., Ding, S.J., 2014. Biosens. Bioelectron. 62, 274–279.
Dragan, A.I., Pavlovic, R., McGivney, J.B., Casas-Finet, J.R., Bishop, E.S., Strouse, R.J., Schenerman, M.A., Geddes, C.D., 2012. J. Fluoresc. 22, 1189–1199.
Feng, X.L., Duan, X.R., Liu, L.B., An, L.L., Feng, F.D., Wang, S., 2008. Langmuir. 24, 12138–12141.
Feng, X.L., Liu, L.B., Yang, Q., Wang, S., 2011. Chem. Commun. 47, 5783–5785.
Ganguly, A., Chen, C.P., Lai, Y.T., Kuo, C.C., Hsu, C.W., Chen, K.H., Chen, L.C., 2009. J. Mater. Chem. 19, 928–933.
Igloi, G.L., 1998. Proc. Natl. Acad. Sci. USA 95, 8562–8567.
Jiang, G.X., Susha, A.S., Lutich, A.A., Stefani, F.D., Feldmann, J., Rogach, A.L., 2009. ACS Nano 3, 4127–4131.
Kang, M., Nag, O.K., Hwang, S., Kim, I., Yang, H., Kyhm, K., Woo, H.Y., 2010. Phys. Chem. Chem. Phys. 12, 15482–15489.
Kang, M., Nag, O.K., Nayak, R.R., Hwang, S., Suh, H., Woo, H.Y., 2009. Macromolecules 42, 2708–2714.
Lee, J., Park, I., Jung, E., Lee, Y., Min, D.H., 2014. Biosens. Bioelectron. 62, 140–144.
Lee, K., Maisel, K., Rouillard, J.M., Gulari, E., Kim, J., 2008. Chem. Mater. 20, 2848–2850.
Li, X.F., Yang, L.O., Cai, X.H., Huang, Y.Q., Feng, X.M., Fan, Q.L., Huang, W., 2013. Biosens. Bioelectron. 41, 218–224.
Lin, C.S., Chen, Y.Y., Cai, Z.X., Zhu, Z., Jiang, Y.Q., Yang, C.Y.J., Chen, X., 2015. Biosens. Bioelectron. 63, 562–565.
Liu, B., 2008. Biosens. Bioelectron. 24, 756–760.
Liu, B., Bazan, G.C., 2004. J. Am. Chem. Soc. 126, 1942–1943.
Liu, Z.W., Wang, H.L., Cotlet, M., 2014. Chem. Mater. 26, 2900–2906.
Ma, D.L., He, H.Z., Leung, K.H., Zhong, H.J., Chan, S.H.D., Leung, C.H., 2013. Chem. Soc. Rev. 42, 3427–3440.
Pu, K.Y., Liu, B., 2009. Adv. Funct. Mater. 19, 1371–1378.
Qiu, B., Guo, L.H., Guo, C.H., Guo, Z.Y., Lin, Z.Y., Chen, G.N., 2011. Biosens. Bioelectron. 26, 2270–2274.
Rosi, N.L., Giljohann, D.A., Thaxton, C.S., Lytton-Jean, A.K.R., Han, M.S., Mirkin, C.A., 2006. Science 312, 1027–1030.
Sefah, K., Tang, Z.W., Shangguan, D.H., Chen, H., Lopez-Colon, D., Li, Y., Parekh, P., Martin, J., Meng, L., Phillips, J.A., Kim, Y.M., Tan, W.H., 2009. Leukemia 23, 235–244.
Tian, N., Tang, Y.L., Xu, Q.H., Wang, S., 2007. Macromol. Rapid. Commun. 28, 729–732.
Wang, B., Yang, Q., Liu, L.B., Wang, S., 2011. Colloid Surface B. 85, 8–11.
Wang, C., Tang, Y.L., Liu, Y., Guo, Y., 2014. Anal. Chem. 86, 6433–6438.
Wang, G.J., Bobkov, G.V., Mikhailov, S.N., Schepers, G., Van Aerschot, A., Rozenski, J., Van der Auweraer, M., Herdewijn, P., De Feyter, S., 2009. ChemBioChem. 10, 1175–1185.
Xiang, D.S., Zhou, G.H., Luo, M., Ji, X.H., He, Z.K., 2012. Analyst 137, 3787–3793.
Xu, H., Gao, S.L., Yang, Q., Pan, D., Wang, L.H., Fan, C.H., 2010. ACS Appl. Mater. Inter. 2, 3211–3216.
Xu, H., Wu, H.P., Huang, F., Song, S.P., Li, W.X., Cao, Y., Fan, C.H., 2005. Nucleic Acids Res. 33, e83.
Yang, L.Y., Zhao, M., Zhang, R.C., Dong, J., Zhang, T., Zhan, X.W., Wang, G.J., 2012. ChemPhysChem. 13, 4099–4104.
Zhang, H.Y., Zhou, D.J., 2012. Chem. Commun. 48, 5097–5099.
Zhang, R.C., Yang, L.Y., Zhao, M., Dong, J., Dong, H.F., Wen, Y.Q., Zhan, X.W., Yang, H., Wang, G.J., 2013. Polymer 54, 1289–1294.
Zhao, M., Yang, L.Y., Zhang, R.C., Dong, J., Dong, H.F., Wen, Y.Q., Zhan, X.W., Wang, G., Lu, Y.F., Wang, G.J., 2013. Polymer 54, 297–302.
Zheng, A.H., Luo, M., Xiang, D.S., Xiang, X., Ji, X.H., He, Z.K., 2013a. Talanta 114, 49–53.
Zheng, J., Zhu, G.Z., Li, Y.H., Li, C.M., You, M.X., Chen, T., Song, E.Q., Yang, R.H., Tan, W. H., 2013b. ACS Nano 7, 6545–6554.
Zhu, J., Lu, Y., Deng, C., Huang, G.L., Chen, S.Y., Xu, S.K., Lv, Y., Mitchelson, K., Cheng, J., 2010. Anal. Chem. 82, 5304–5312.